Electronic Band Systems of SF 2 Radicals Observed by Resonance-Enhanced Multiphoton Ionization

ARTICLE *in* THE JOURNAL OF PHYSICAL CHEMISTRY A · SEPTEMBER 1998

Impact Factor: 2.69 · DOI: 10.1021/jp981769p

Electronic Band Systems of SF_2 Radicals Observed by Resonance-Enhanced Multiphoton Ionization

Quanxin Li, Jinian Shu, Qun Zhang, Shuqin Yu, Limin Zhang, Congxiang Chen, and Xingxiao Ma*

Key Laboratory for Bond-selective Chemistry, Chinese Academy of Sciences, and Department of Chemical Physics, University of Science and Technology of China, Hefei, Anhui 230026, Peoples' Republic of China

Received: April 8, 1998; In Final Form: June 15, 1998

A pulsed dc electric discharge in a pulsed supersonic beam has been used as an efficient source of producing radicals. The (2+1) REMPI spectra of the SF_2 radicals were investigated between 245 and 365 nm (54945−81630 cm^{-1}). Eight electronic band systems have been observed in this range. One series with quantum defect $\delta = 1.961(6)$ is comprised of the $\tilde{B}\ ^1B_1(4s)$ and $\tilde{J}\ ^1B_1(5s)$ Rydberg states which have origins at $\nu_{0-0} = 54470$ and 68951 cm^{-1}, respectively. Vibrational analyses of these Rydberg states showed that in the $\tilde{B}\ ^1B_1(4s)$ state $\omega_1'(a_1$ sym str) = 981(23) cm^{-1} and in the $\tilde{J}\ ^1B_1(5s)$ state $\omega_1'(a_1$ sym str) = 942(3) cm^{-1}. A second Rydberg series $\tilde{E}$ (4p) with quantum defect $\delta = 1.61$ is characterized with the spectroscopic values $\nu_{0-0} = 62025\ cm^{-1}$, $\omega_1'(a_1$ sym str) = 941(27) cm^{-1}, and $\omega_2'(a_1$, bend) = 413(12) cm^{-1}. Incompletely rotational analysis revealed that the $\tilde{F}$ electronic state with $\nu_{0-0} = 63812\ cm^{-1}$, $\omega_1'(a_1$ sym str) = 966(6) cm^{-1}, and $\omega_2'(a_1$, bend) = 417(23) cm^{-1} merges with the vibrational progression of the $\tilde{E}$ (4p) state. The $\tilde{F}$ state might be a 4p Rydberg state of another hybrid symmetry with the quantum defect $\delta = 1.50$. A third Rydberg series is comprised of the $\tilde{G}$ (3d) ($\nu_{0-0} = 68378\ cm^{-1}$, $\omega_1' = 939(12)\ cm^{-1}$, $\delta = 0.086$), the $\tilde{H}$ (3d) ($\nu_{0-0} = 68571\ cm^{-1}$, $\omega_1' = 936(4)\ cm^{-1}$, $\delta = 0.064$), and the $\tilde{I}$ (3d) ($\nu_{0-0} = 68847\ cm^{-1}$, $\omega_1' = 933(4)\ cm^{-1}$, $\delta = 0.032$). In addition, two valence states labeled as the $\tilde{B}'$ state (38623 cm^{-1}) and $\tilde{C}$ state (56219−61278 cm^{-1}) were also observed. A fit of the Rydberg formula to the $ns(^1B_1)$ ($n = 4,5$) origins found the adiabatic ionization potential of SF_2 radicals to be $IP_a = 10.021(1)$ eV.

Introduction

Resonance-enhanced multiphoton ionization (REMPI) spectroscopy of transient free radicals has been developed for ∼20 years. Due to the major appealing features of REMPI spectroscopy, such as high sensitivity and less restrictive selection rules compared with laser induced fluorescence, this method has played a significant role in the studies of electronic structures and chemical kinetic processes for free radicals. The REMPI spectroscopic results of many free radicals have been well reviewed by Hudgens[1] and Ashfold et al.[2] In this paper, we present a "laser-free" method to generate free radicals by using a pulsed dc electric discharge in a supersonic gas mixtures. The use of an electric discharge for preparation of the transient species is a traditional technique, which has proved to be a powerful tool for the spectroscopic studies.[3−10] As pointed out by Sharp and Johnson,[4] however, the greatest obstacle to this method was its instabilities and a large amount of background ions produced by the discharge. Formation of a stable discharge in a pulsed beam is very difficult because of the rapidly varying gas density.[4]

Interest in the SF_2 radical has increased because of its potential importance in semiconductor manufacturing. It is believed that SF_2 radicals play a significant role in plasma etching by SF_6/O_2.[11−14]

Most previous experimental studies have been focused upon the investigation of the ground-state properties of SF_2 radical. The microwave spectroscopic measurements have established that SF_2 possesses a planar C_{2v} structure with a bond length $r(S-F) = 1.59$ Å and a bond angle $\theta(F-S-F) = 98.27°$.[15−17] The three vibrational frequencies of SF_2 ($\tilde{X}^1A_1$) (i.e., $\omega_1''(a_1$ sym str), $\omega_2''(a_1$ bend) and $\omega_3''(b_1$ asym str)) have been determined by infrared spectra,[18−20] microwave spectrum,[16] and chemiluminescence measurements.[21] The rotational constants of SF_2 ($\tilde{X}^1A_1$) have also been obtained by the microwave spectra.[15,16] The equilibrium geometries of the ground state and lower excited electronic states of SF_2^+ all belong to the C_{2v} point group. The adiabatic ionization potential ($IP_a(SF_2) = 10.08$ eV), and ω_1' of $SF_2^+(X^2B_1)$ (935(40) cm^{-1}), have been measured by gas-phase photoelectric spectroscopy.[22] The lowest six excited electronic states of SF_2^+ have also been observed.[22]

In contrast, previous spectroscopic and structural information about the excited electronic states of neutral SF_2 radical was limited. The chemiluminescence between 550 and 860 nm in the reaction of F_2 with CS_2 has been ascribed to the transition of the $SF_2(\tilde{A} - \tilde{X})$.[21] The 4s ($\tilde{B}^1B_1$) and the 4p($\tilde{E}$) Rydberg states of SF_2 radical have been identified by the pioneering REMPI work of Johnson and Hudgens.[23] The spectral data, including the vibrational frequencies and the band origins of 4s and 4p Rydberg states have been determined.[23] In addition, a valence state which overlaps the vibrational progression of 4s Rydberg state was also observed. Even so, some uncertainties associated with the excited electronic states of SF_2 radicals also remain. For example, how to explain the irregular vibrational intervals along the ω_1' symmetric stretching appeared in the 4p Rydberg state? How to make it clear for the detailed spectroscopic information of the valence state mentioned above? Furthermore, discoveries of other new excited electronic states for this radical should be a challenge.

* To whom all correspondence should be addressed.

S1089-5639(98)01769-1 CCC: $15.00
Published on Web 08/25/1998

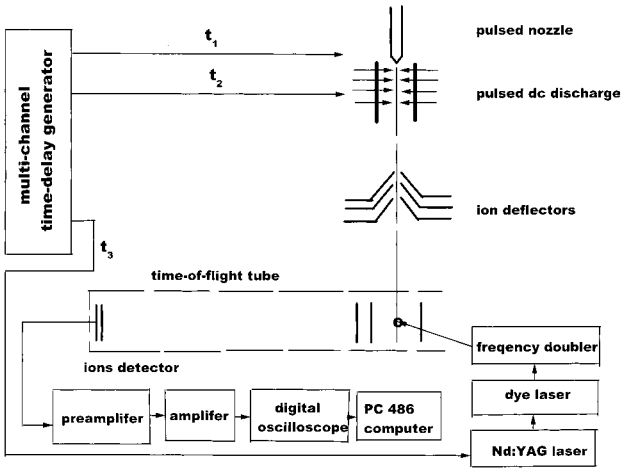

Figure 1. Schematic diagram of the radical REMPI experimental setup, in which a pulsed dc discharge in the supersonic beam was used to generate free radicals.

In this paper we present a "laser-free" pulsed radical source. SF_2 radicals were produced by a dc electric discharge of a supersonically expanding gas mixture of SF_6 and Argon. The electronic spectra of SF_2 radicals from 54795 cm^{-1} up to its ionization potential (81300 cm^{-1}) have been investigated by REMPI spectroscopy. Eight electronic band systems were observed, in which, as we know, five electronic states were first detected. Special attentions have been paid to 4p Rydberg state. A new electronic state overlapping with the vibrational progression of 4p Rydberg state was identified by incompletely rotational analysis. Finally, a clearer scheme of electronic band systems of SF_2 radical has been presented.

Apparatus and Method

A schematic diagram of the experimental apparatus used in this work is shown in Figure 1. It consists of a radical generation source, a pulsed Nd:YAG-pumped frequency-doubled dye laser, an ion detector, and a computer data acquisition system.

SF_2 radicals were generated by the pulsed dc discharge in a pulsed supersonic beam of Ar seeded with SF_6 (30%). The molecular beam formed through a pulsed injection valve of 1 mm diameter. The stagnation pressure was monitored from 1.5 to 3 atm. In order to produce a stable discharge in the pulsed supersonic beam, a discharge design based on some laser discharge modes (such as excimer laser or pulsed TEA CO_2 laser) was adopted. The pulsed dc electric discharge (at 1500−3000 V in 10 μs/pulse width) was initiated between the four pairs of tungsten needles, and stable glow discharge was created between a pair of parallel copper plates. The background ions produced by the discharge were effectively eliminated by two reflectors, which consisted of three skimmers with the same diameter of 1 mm. The first skimmer was located downstream from the nozzle of 10 cm, and the interval between two skimmers is 5 mm. The electric potentials applied to the ion reflectors were chosen as low as possible. The photoionization chamber was maintained at a typical pressure of $5-10 \times 10^{-5}$ Torr under the operating conditions. A multi-channel delay generator controlled the relative time delays among the nozzle, the dc discharge, and the laser.

The light source used was a dye laser (Lumonics: HT500) pumped with either the second (at 532 nm) or the third (at 355 nm) harmonic of the Nd:YAG laser (Spectra Physics: GCR-170). The dye laser output was frequency-doubled with a doubler (Lumonics HT1000). Presented in Table 1 are the Nd:YAG pump wavelengths, laser dyes, and wavelength region covered by each dye. The frequency-doubled laser (1−2 mJ/pulse, bandwidth ∼0.08 cm^{-1} fwhm) was focused by a lens (f = 300 mm) into the photonionization zone. The dye laser wavelength was scanned in the increment of ∼0.02−0.0001 nm/s. The wavelength of the laser fundamental was calibrated against known neon and argon atomic transitions using opto-galvanic spectroscopy.[24−25] The ions generated by REMPI processes were detected by a usual time-of-flight mass spectrometer. The ion signal from the mass spectrometer was amplified by an amplifier (NF Electron Corp: BX231A), recorded using a digitizer (Kikusui: 710A), and then averaged with a PC486 computer data acquisition system.

TABLE 1: The Pump Laser Wavelength, the Laser Dyes, Their Spectral Range, and Maximum Energies Used During This Study

pump laser wavelength, nm	dye	wavelength range, nm	maximum energy, mJ/pulse
532	LDS698	664−755	2
532	DCM	616−678	2
532	R640	621−674	2
532	KR620	594−641	2
532	R610	588−632	2
355	R590	563−597	2
355	C540A	523−587	2
355	C485	499−565	2
355	C500	481−550	2
355	C480	458−507	2

The REMPI excitation spectra were obtained by measuring the m/z 70 ($^{32}SF_2^+$) ion signal as a function of laser wavelength. The presented spectral intensity has not been calibrated by the dye laser intensity. Whenever possible, proper relative intensities across the REMPI spectra were maintained by comparison of band intensities in regions where the different dye wavelength ranges overlapped. The gas samples used in this work were SF_6 (99.99%) and argon (99.999%). The entire experimental apparatus and method used for the present REMPI studies of free radicals have proved reliable by carefully observing the known rotationally resolved spectra of SO, CF, and CH_3 radicals, which were produced by the pulsed dc discharge of $SOCl_2$/Ar, CF_4/Ar or CF_2Cl_2/Ar, and CH_3I/Ar mixtures, respectively.

Results and Analyses

A. Identification of the Spectral Carrier. In this study, SF_2 radicals were generated by the pulsed dc discharge in the mixtures of SF_6 and argon. Three typical mass spectra, shown in Figure 2, were investigated in the cases: (a) the dc discharge alone, (b) the 322.45 nm laser irradiation alone, and (c) the dc discharge together with the 322.45 nm laser irradiation. As shown in Figure 2, the strong $^{32}SF_2^+$ (m/z = 70) ion signal appeared only in the case (c). We therefore believe that the signal of SF_2^+ should be contributed directly to neither the discharge nor the products of multiphoton ionization with photodecomposition of parent molecule SF_6. Furthermore, the spectral assignments strongly support that the excitation spectra originate from a two-photon resonance transition followed by a one-photon ionization of neutral SF_2 radicals, which are most like from the discharge of SF_6, since the vibrational progressions associated with 4s and 4p Rydberg states observed here agree quite well with the previous observation by Johnson and Hudgens.[23]

B. REMPI Spectrum of SF_2 Radical between 295−325 nm. Figure 3 displays the vibrationally resolved REMPI

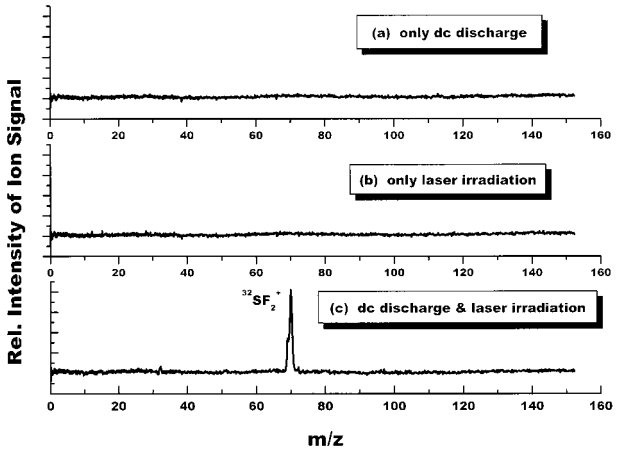

Figure 2. Three typical mass spectra under the conditions: (a) the dc discharge alone, (b) the 322.45 nm laser irradiation alone, and (c) the dc discharge together with the 322.45 nm laser irradiation. The $^{32}SF_2^+$ (m/z 70) ion signals appeared only in the case (c).

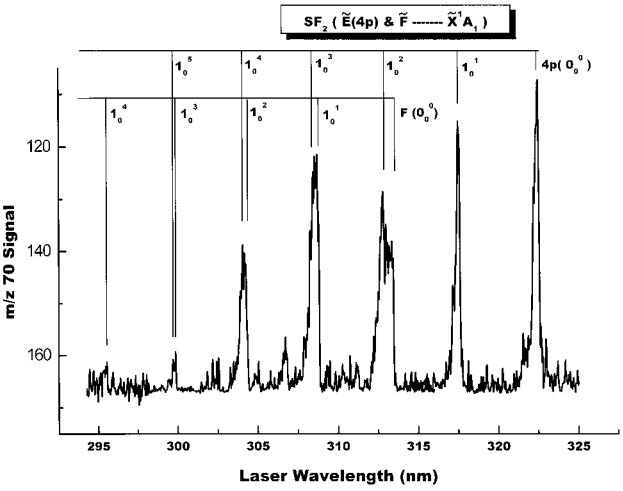

Figure 3. The composite REMPI spectrum of the $^{32}SF_2$ radical observed between 295 and 325 nm.

spectrum of SF_2 between 295 and 325 nm. Since multiphoton experiments may have more than one possible excitation mechanism, a correct determination of the photon order of the resonant state is very important to assign the REMPI spectra and derive related spectroscopic constants. In this paper, we used several approaches to determine the photon order of resonant transitions observed in the SF_2 radical spectra. First, the vibrational analyses of each electronic state, considered as a reliable approach, can be used to establish the photon order of each band system.[26−29] Second, quantum defect of the Rydberg state is an important factor to judge the photon order of the Rydberg series. Quantum defect (δ) may vary only within a limited range for each orbital type. For example, for sulfur-centered Rydberg orbitals, the δ values of the *n*s, *n*p, *n*d, and *n*f Rydberg states should lie near 2.0, 1.6, 0.08, and 0.06, respectively.[30] Quantum defect can be derived by the familiar Rydberg formula:

$$\nu_{0-0}(\mathrm{cm}^{-1}) = \mathrm{IP_a} - 109737/(n-\delta)^2$$

where ν_{0-0} is the electronic state origin, IP_a is the adiabatic ionization potential in cm^{-1} (for SF_2, $IP_a = 81301\ cm^{-1}$ [22]), n is the principal quantum number, and δ is the quantum defect. Third, if possible, the analyses of vibrational hot bands which reflect a spectroscopic information of the ground state are also employed to identify the photon order.

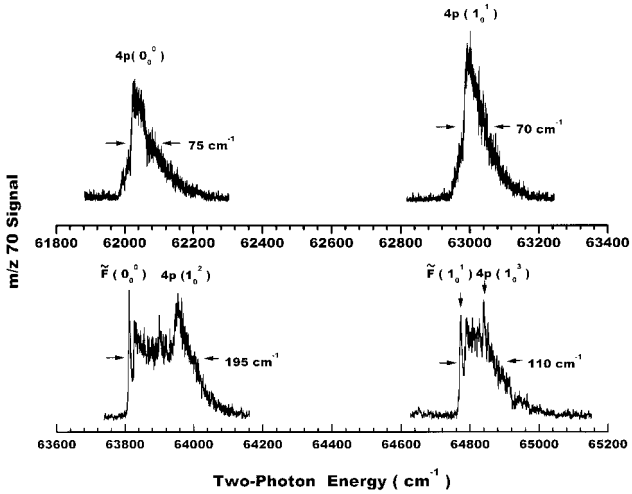

Figure 4. The incompletely rotationally resolved (2+1) REMPI spectrum of the $^{32}SF_2$ radical between 61800 and 65000 cm^{-1}.

In Figure 3, the REMPI spectrum of SF_2 radicals between 295 and 325 nm displays five strong peaks (band maxima) in the wavelengths of 322.45, 317.54, 312.78, 308.17, and 304.06 nm, respectively. The longest wavelength band of this intense progression lies at 322.45 nm. Using the Rydberg formula, this band can be attributed to a two-photon resonant transition from the ground state to the Rydberg state with $n = 4$ and $\delta = 1.61$. Since this quantum defect is a proper magnitude for p orbital Rydberg states,[30] we can arrive at that the band origin of the 4p Rydberg state lies at 62025 cm^{-1}.

In C_{2v} symmetry, the vibrational selection rules in the Born−Oppenheimer approximation are $\Delta v = 0, \pm1, \pm2, \ldots$ for the normal mode of a_1 symmetry and $\Delta v = 0, \pm2, \pm4, \ldots$ for the normal modes of a_2, b_1, and b_2 symmetries.[31] We initially expected that all prominent peaks arised from a vibrational progression of the 4p Rydberg state associated with ω_1'(a_1 sym str) vibrational mode. However, the bands of 4p Rydberg state appear as irregular intervals of $2h\nu = 959$, 959, 830, and 1003 cm^{-1}. Careful inspection shows that the bands of 4p(0_0^0) and 4p(1_0^1) distinguish from the others. Figure 4 presents incompletely rotationally resolved spectra (scanned increment of 0.0001 nm/s) for the first four vibrational peaks. The shape and the width (fwhm) of the 4p(0_0^0) and 4p(1_0^1) bands are very similar. In contrast, the 4p(1_0^2) and 4p(1_0^3) bands exhibit a distinct broadening and shape changing. The broadened bands may originate from the activity of the ω_3(b_1 asym str) vibrational mode, or the combination bands between the ω_1(a_1, sym str) and ω_3(b_1, asym str) vibrational modes (i.e., $1_0^m3_0^n$). In this way, the first five profiles should be assigned as 4p(0_0^0), 4p(1_0^1), 4p(1_0^2, 3_0^2), 4p(1_0^3, $1_0^13_0^2$), and 4p(1_0^4, $1_0^23_0^2$, 3_0^4). Unfortunately, this approach cannot be reasonable because the fifth profile is not the widest one as expected. Similarly, the examination of combination bands of $1_0^m3_0^n$ also failed. Other alternative explanations, such as spin−orbit splitting, Fermi-resonance, and John−Teller interaction, etc., were all in failure in the present case. Thus, the properties of the spectrum observed here seem to reflect the presence of another excited electronic state accompanying with the 4p Rydberg state, as previously predicted by Johnson and Hudgens.[23]

The spectrum between 295 and 325 nm arises from two excited electronic states labeled as $\tilde{E}$ (4p) and $\tilde{F}$. We assign the prominent vibrational progressions of the $\tilde{E}$ and $\tilde{F}$ states to the ω_1'(a_1 sym str) vibration. Analysis of the ω_1' band intervals in the $\tilde{E}$ (4p) state presents the spectroscopic values: $\omega_1' = 941(27)$ cm^{-1} and $T_0 = 62025$ cm^{-1}. On the basis of the

TABLE 2: Band Positions, Assignments, and Spacings Observed in the REMPI Spectrum of $^{32}SF_2$ (m/z = 70) Radical between 295 and 325 nm

assignment	band pos (λ_{air}), nm	state energy, cm^{-1}	energy relative to E (4p 0_0^0), cm^{-1}	energy relative to $\tilde{F}$ (0_0^0), cm^{-1}	ω_1 band interval, cm^{-1}	ω_2 band interval, cm^{-1}
4p 0_0^0	322.45	62025	0			
4p 2_0^1	320.35	62432	407			407
4p 1_0^1	317.54	62984	959		959	
4p $1_0^1 2_0^1$	315.53	63385	1360			401
$\tilde{F}$ 0_0^0	313.42	63812		0		
4p 1_0^2	312.78	63943	1918		959	
$\tilde{F}$ 2_0^1	311.33	64241		429		429
4p $1_0^2 2_0^1$	310.72	64367	2342			424
$\tilde{F}$ 1_0^1	308.77	64773		961	961	
4p 1_0^3	308.46	64838	2813		895	
$\tilde{F}$ $1_0^1 2_0^1$	306.72	65206		1394		433
4p $1_0^3 2_0^1$	306.56	65240	3215			402
$\tilde{F}$ 1_0^2	304.25	65735		1923	962	
4p 1_0^4	304.06	65777	3752		939	
$\tilde{F}$ $1_0^2 2_0^1$	302.41	66135		2323		400
4p $1_0^4 2_0^1$	302.16	66190	4165			413
$\tilde{F}$ 1_0^3	299.84	66702		2890	967	
4p 1_0^5	299.72	66729	4704		952	
$\tilde{F}$ 1_0^4	295.53	67675		3863	973	

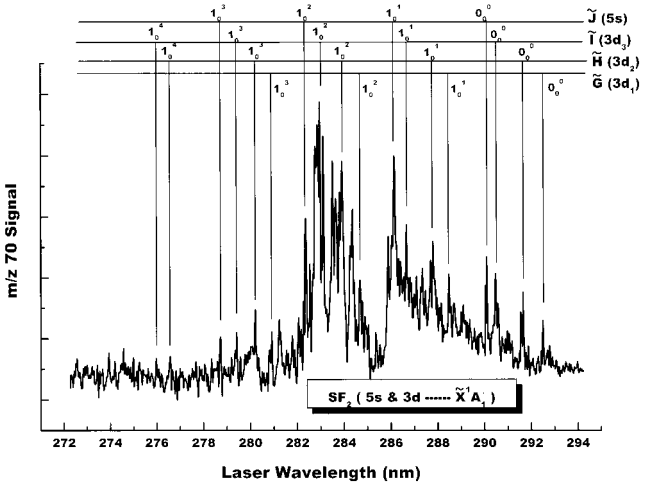

Figure 5. The composite REMPI spectrum of the $^{32}SF_2$ radical observed between 272 and 295 nm.

analysis of the fine spectrum (see Figure 4), the $\tilde{F}$ state has been assigned with the values: $\omega_1' = 966(6)$ cm^{-1} and $T_0 = 63812$ cm^{-1}. Many weak bands observed between 295 and 325 nm are described by 2_0^1 band and $1_0^n 2_0^1$ (n = 1,2, ...) combination bands of the $\tilde{E}$ (4p) and $\tilde{F}$ states, from which the vibrational frequencies of $\omega_2'(a_1$ bend) = 413(12) cm^{-1} and 417(23) cm^{-1} for the $\tilde{E}$ (4p) and $\tilde{F}$ states, respectively, have been derived. Table 2 summaries the band positions, assignments, and spacings observed in the REMPI spectrum of $^{32}SF_2$ radical between 295 and 325 nm.

The adiabatic ionization potential (IP_a = 10.08 eV (81301 cm^{-1})) of SF_2 radical has been measured by PES.[22] To form the $^{32}SF_2^+$ ion, the SF_2 radical in the $\tilde{E}$ (4p) or $\tilde{F}$ states must absorb a third laser photon. This excitation scheme is commonly referred to a (2+1) REMPI mechanism. The explanation of the REMPI spectra is impossible using mechanism other than 2+1. In addition, only $^{32}SF_2^+$ ions appeared over the range of 295−325 nm. Thus, the SF_2^+ ions may not fragment.

C. REMPI Spectrum of SF_2 between 272−294 nm. Figure 5 presents the REMPI spectrum of SF_2 radical between 272 and 294 nm. The spectrum shows four prominent progressions, labeled as $\tilde{G}$, $\tilde{H}$, $\tilde{I}$, $\tilde{J}$, which possess average vibrational intervals of 939, 936, 933 and 942 cm^{-1}, respectively. Table 3 lists the band positions, assignments, two-photon energies, and band intervals of these progressions. Using the similar analyses as described above for the $\tilde{E}$ (4p) Rydberg state, we have assigned these progressions to the activities of the $\omega_1'(a_1$ sym str) modes of the four Rydberg states. The termination of the vibrational progression at 290.06 nm ($2h\nu$ = 68951 cm^{-1}) is the electronic origin of the $\tilde{J}$ state. This origin falls within the range predicted for a 5s Rydberg state. Using this origin assignment and the adiabatic ionization (IP_a = 81301 cm^{-1}) for SF_2 to solve the Rydberg equation, we find a quantum defect of δ = 2.01, which is a reasonable value for the *n*s-type Rydberg states.[30] We assign the $\tilde{G}$ state origin to lie within the congested band at 292.49 nm ($2h\nu$ = 68378 cm^{-1}), which is described as a 3d Rydberg state with n = 3, δ = 0.086. The origins of the $\tilde{H}$ and $\tilde{I}$ states locate at 291.67 nm ($2h\nu$ = 68571 cm^{-1}) and 290.50 nm ($2h\nu$ = 68847 cm^{-1}), respectively. Since no Rydberg states other than 3d and 5s states are expected to fall within the present energy range, the $\tilde{H}$ and $\tilde{I}$ states might be the 3d Rydberg states with different symmetries from that of the $\tilde{G}$ state. On the basis of the Rydberg formula, the quantum defects of the $\tilde{H}$ and $\tilde{I}$ states are 0.064 and 0.032, respectively.

According to the assignments of the vibrational progressions appeared in the REMPI spectrum between 272−294 nm, the vibrational frequencies $\omega_1'(a_1$ sym str) of 939(12), 936(4), 933-(4), and 942(3) cm^{-1} for the $\tilde{G}$, $\tilde{H}$, $\tilde{I}$, and $\tilde{J}$ Rydberg states, respectively, can be yielded. We find that these values are very similar to the $\omega_1(a_1$ sym str) of 935(45) cm^{-1} for the SF_2 cation.[22] This result is not surprising because the high Rydberg electron usually interacts weakly with the ionic core, the bonding and mechanic motion of the Rydberg molecule is almost the same as that in the cation. In this way, the vibrational properties of high Rydberg states may be close to those of cation.

The regularity of the $\omega_1'(a_1$ sym str) vibrational intervals and the reasonable quantum defects derived for the $\tilde{G}$, $\tilde{H}$, $\tilde{I}$, and $\tilde{J}$ Rydberg states support our assignment of the REMPI spectrum between 272−294 nm to two-photon resonance with these Rydberg states of the SF_2 radical. The alternate assignments to one-photon resonance could not explain the spectrum presented in Figure 5. Noticing that the SF_2 radical must absorb three photons to be ionized and to form the SF_2^+ ($\tilde{X}$) in this

TABLE 3: Band Positions, Assignments, and Spacings Observed in the REMPI Spectrum of $^{32}SF_2$ (m/z = 70) Radical between 275 and 295 nm

assignment	band position (λ_{air}), nm	state energy, cm^{-1}	energy relative to $\tilde{G}$ (0_0^0), cm^{-1}	energy relative to $\tilde{H}$ (0_0^0), cm^{-1}	energy relative to $\tilde{I}$ (0_0^0), cm^{-1}	energy relative to $\tilde{J}$ (0_0^0), cm^{-1}	ω_2 band interval, cm^{-1}
$\tilde{G}$ 0_0^0	292.49	68 378	0				
$\tilde{H}$ 0_0^0	291.67	68 571		0			
$\tilde{I}$ 0_0^0	290.50	68 847			0		
$\tilde{J}$ 0_0^0	290.06	68 951				0	
$\tilde{G}$ 1_0^1	288.59	69 326	948				948
$\tilde{H}$ 1_0^1	287.74	69 507		936			936
$\tilde{I}$ 1_0^1	286.63	69 776			929		929
$\tilde{J}$ 1_0^1	286.15	69 893				942	942
$\tilde{G}$ 1_0^2	284.69	70 252	1874				926
$\tilde{H}$ 1_0^2	283.90	70 447		1876			940
$\tilde{I}$ 1_0^2	282.84	70 711			1864		935
$\tilde{J}$ 1_0^2	282.36	70 832				1881	939
$\tilde{G}$ 1_0^3	280.92	71 195	2817				943
$\tilde{H}$ 1_0^3	280.18	71 383		2812			936
$\tilde{I}$ 1_0^3	279.15	71 646			2799		935
$\tilde{J}$ 1_0^3	278.64	71 777				2826	945
$\tilde{H}$ 1_0^4	276.57	72 314		3743			931

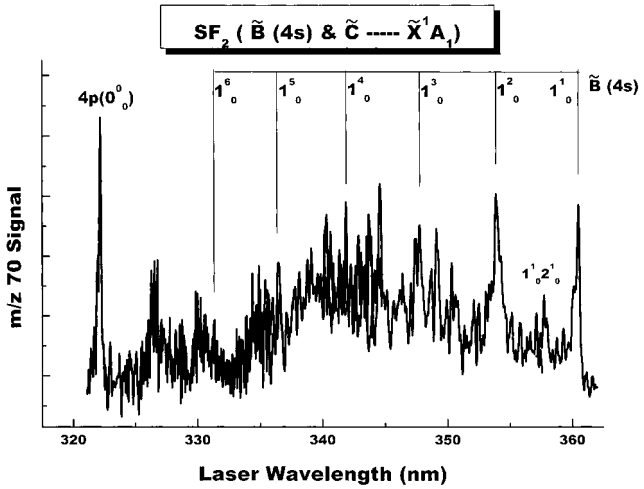

Figure 6. The composite REMPI spectrum of the $^{32}SF_2$ radical observed between 320 and 365 nm.

wavelength range, therefore, we attribute the REMPI spectrum to a (2+1) REMPI mechanism. Other REMPI bands appearing at 281.24, 283.52, 284.34, 287.34, 289.07, and 290.97 nm, have no firm spectroscopic assignments in this paper. They may originate from the excitation of other modes and/or the combination bands between the ω_1'(a_1 sym str) mode and the unassigned modes.

D. REMPI Spectrum of SF_2 Radical between 320 and 365 nm. Figure 6 presents the REMPI spectrum of SF_2 between 320 and 365 nm. The REMPI spectrum displays a number of bands which emerge into a continuous profile. This continuous vibrational contour in present energy range may suggest that the upper state suffer from predissociation or rapid nonradiative decay. Either process could quench REMPI signal of the SF_2^+.[1,2] In contrast to the $\tilde{E}$ (4p) and $\tilde{F}$ states, the fragmental ions $^{32}SF^+$ (m/z = 51) and $^{32}S^+$ (m/z = 32) have been observed between 320 and 360 nm. This evidence supports the explanation of the continuous profile. It should be pointed out that whenever the pulsed dc discharge which generated the SF_2 radicals was extinguished, the REMPI signals of the $^{32}SF_2^+$ (m/z = 70), $^{32}SF^+$ (m/z = 51) and $^{32}S^+$ (m/z = 32) ions all disappeared. Thus, the fragmental ions were not formed by the photodissociation of the SF_6 molecules,which was followed by the REMPI ionization.

Two excited electronic states, labeled as $\tilde{B}$ and $\tilde{C}$ states, have been identified in the REMPI spectrum of the SF_2 radical between 320 and 365 nm. The spectrum in Figure 5 displays an intense progression of the $\tilde{B}$ state, which appears at 360.68, 354.22, 348.02, 342.14 and 336.69, and 331.37 nm. This progression arises from a series of 1_0^n (n = 1−6) fundamental bands. The $\tilde{B}$ state was first observed by (2+1) REMPI spectra between 330−370 nm and described as the 4s Rydberg state.[23] Table 4 lists the band positions, assignments, and spacings observed by present (2+1) REMPI spectrum in the range of 325−365 nm. Within the experimental measurement uncertainties, the vibrational band positions and frequency intervals presented here agree very well with those observed by Johnson and Hudgens.[23] A vibrational analysis of the $\tilde{B}$ (4s) state observed here gives the spectroscopic values: ω_1'(a_1 sym str) = 981(23) cm^{-1}, ω_2'(a_1 bend) = 388(24) cm^{-1}. Unfortunately, the laser wavelength longer than 365 nm was not able to reach because we have no available frequency-doubled crystal temporally. Accordingly, the band origin of $\tilde{B}$ (4s) was not measured in this account.

Another excited electronic state, labeled as $\tilde{C}$ here, also reside in this wavelength range. This band system appears as an irregular series of closely spaced bands from 326.38 to 355.75 nm ($2h\nu$ = 56219−61278 cm^{-1}). In Table 4, the band positions and state energies of the $\tilde{C}$ state were presented. Johnson and Hudgens[23] also observed the $\tilde{C}$ state (336−350 nm) and suggested this state might be a valence state (57000−60000 cm^{-1}) with the configuration and symmetry ... $1a_2^2 5b_2^2 8a_1^2$-$3b_1^1 6b_2^1$ ($^1A_2$). Between 320 and 365 nm SF_2 radical must absorb three photons to ionize and form the SF_2^+. Thus, it seems that the $\tilde{C}$ state is a two-photon resonant state and the SF_2^+ ions are generated by (2+1) REMPI process. The REMPI spectrum observed in this range has not been reasonably assigned.

E. REMPI Spectrum of SF_2 Radicals between 245 and 275 nm. Figure 7 shows the mass-resolved REMPI spectrum of the SF_2 radical in the wavelength range of 260−275 nm. The spectrum displays two obvious broad profiles with the central wavelength at 266.8 and 269.5 nm. An extremely weak REMPI spectrum was also observed between 245 and 260 nm and not showed in Figure 7.

The envelopes labeled as I and II in Figure 7 do not result from the variant of the dye laser intensity, because the relative

TABLE 4: Band Positions, Assignments, and Spacings Observed in the REMPI Spectrum of $^{32}SF_2$ (m/z = 70) Radical between 325 and 360 nm

assignment	band position (λ_{air}), nm	state energy, cm^{-1}	energy relative to $\tilde{B}$ (4s 1_0^1), cm^{-1}	ω_1 band interval, cm^{-1}	ω_2 band interval, cm^{-1}
4s 1_0^1	360.68	55 451	0		
4s $1_0^1 2_0^1$	358.12	55 847	396		396
4s 1_0^2	354.22	56 462	1011	1011	
4s $1_0^2 2_0^1$	351.72	56 863	1412		401
4s 1_0^3	348.02	57 468	2017	1006	
4s $1_0^3 2_0^1$	345.81	57 835	2384		367
4s 1_0^4	342.14	58 456	3005	988	
4s 1_0^5	336.69	59 402	3951	946	
4s 1_0^6	331.37	60 356	4905	954	
Č	355.75	56 219			
Č	350.50	57 061			
Č	349.34	57 251			
Č	345.81	57 835			
Č	344.76	58 011			
Č	343.90	58 156			
Č	343.11	58 290			
Č	342.47	58 399			
Č	341.52	58 562			
Č	340.50	58 737			
Č	339.36	58 934			
Č	338.34	59 112			
Č	336.20	59 488			
Č	335.62	59 591			
Č	335.12	59 680			
Č	334.10	59 862			
Č	333.23	60 019			
Č	330.86	60 449			
Č	328.95	60 800			
Č	327.94	60 987			
Č	327.05	611 153			
Č	326.71	61 216			
Č	326.38	61 278			

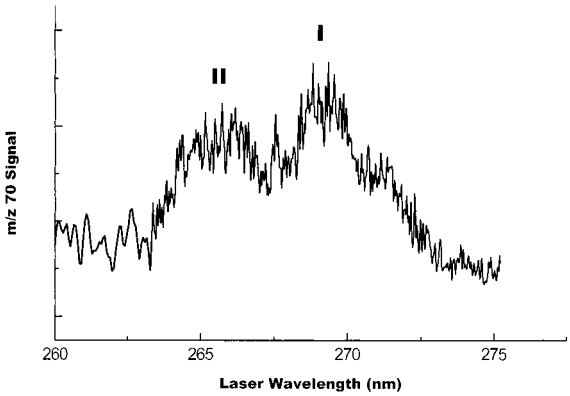

Figure 7. The REMPI spectrum of the $^{32}SF_2$ radical observed between 260 and 275 nm.

laser intensity across this wavelength range changes so slowly that the band contour suffers from little distortion. The spectrum carried by $^{32}SF_2^+$ (m/z = 70) was monitored simultaneously with that carried by $^{32}S^+$ (m/z = 32). Cautious comparison of the $^{32}SF_2^+$ (m/z = 70) spectrum with the $^{32}S^+$ (m/z = 32) spectrum found that the feature of $^{32}SF_2^+$ (m/z = 70) spectrum discussed above also appeared in the $^{32}S^+$ (m/z = 32) REMPI spectrum between 260−275 nm. Therefore, the $^{32}S^+$ signal may originate from the dissociation of the $^{32}SF_2^+$ in this spectrum region.

The spectrum shown in Figure 7 displays very weak resonant structures. An exact assignment of this spectrum was impossible currently. Energetically, the SF_2 radical must absorb three laser photons to form the $^{32}SF_2^+$ between 265−272 nm. The envelopes I and II should originate from a (2+1) REMPI process because no single photon resonant states were observed in this wavelength range. The observed broad resonance shown in Figure 7 might reflect the two-photon resonance enhancement associated with high Rydberg states (e.g., 6s, 4d, or 4f Rydberg states).

Discussion

A. Electronic States of SF_2 Radical. We have observed the (2+1) REMPI spectra of the SF_2 radical and assigned them to originate from eight electronic states that lie between 54795 and 81600 cm^{-1}. The $^{32}SF_2^+$ ions monitored were formed through a (2+1) REMPI process.

Figure 8 diagrams the picture of the known electronic state energy levels of SF_2 radical. The ground state of SF_2 is described in C_{2v} symmetry group with the configuration:

$1a_1^2 2a_1^2 1b_2^2 3a_1^2 1b_1^2 4a_1^2 2b_2^2 5a_1^2 3b_2^2 6a_1^2 2b_1^2 7a_1^2 4b_2^2 1a_2^2 5b_2^2 8a_1^2 3b_1^2$

The Rydberg states investigated by present REMPI spectra are formed by promotion of the $3b_1$ electron into various diffuse Rydberg orbitals with following configurations (in C_{2v}):

$$\ldots 5b_2^2 8a_1^2 3b_1^1 ns^1$$

$$\ldots 5b_2^2 8a_1^2 3b_1^1 np^1$$

$$\ldots 5b_1^2 8a_1^2 3b_1^1 nd^1$$

The SF_2 radical in these Rydberg states may be ionized through the following processes:

$\ldots 5b_2^2 8a_1^2 3b_1^1$ (ns^1, np^1, or nd^1) + $h\nu \rightarrow \ldots 5b_2^2 8a_1^2 3b_1^1$ ($\tilde{X}\ ^2B_1$) + e^-

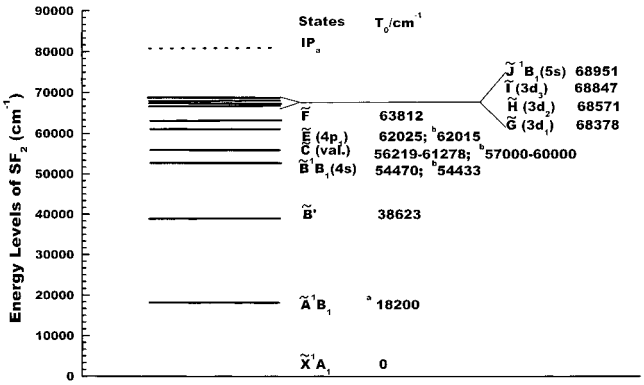

Figure 8. The energy level diagram which shows the known electronic states of SF_2 radical from the ground state up to the ionization potential of SF_2 radical. a) observed by the emission spectrum between 550 and 860 nm in the reaction of F_2 with CS_2 (ref 21). b) observed by the previous REMPI spectra (ref 23).

In Figure 8, $\tilde{B}$ and $\tilde{J}$ represent the 4s and 5s Rydberg states, respectively. The symmetry $^1B_1$ for these *n*s Rydberg series can be derived by the orbitals' symmetry combination. The REMPI spectra reported here do not cover the wavelength range of the band origin $\tilde{B}(0_0^0)$. On the basis of the extrapolation of the observed data, we estimated that the origin of the $\tilde{B}\ ^1B_1(4s)$ Rydberg state should lie at 54470 cm^{-1}. Johnson and Hudgens measured the first REMPI spectrum of the SF_2 radical between 295 and 495 nm.[23] In their study, the SF_2 radicals were produced by a microwave discharge and the reaction of F atom with H_2S/CS_2. Three excited electronic states, namely, 4s, 4p Rydberg states and $\tilde{C}$ state were investigated by their REMPI spectra. They established that the $\tilde{B}\ ^1B_1(4s)$ resides at 54433 cm^{-1}. Although the present extrapolated origin agrees reasonably with theirs, we believe that the band origin of the $\tilde{B}\ ^1B_1$-(4s) ($T_0 = 54433$ cm^{-1}) given by Johnson and Hugens[23] might be more accurate.

This study has identified another *n*s Rydberg state ($\tilde{J}\ ^1B_1$-(5s)). The vibrational analysis and quantum defect support the assertion that the $\tilde{J}\ ^1B_1(5s)$ state lies at 68951 cm^{-1}.

The $\tilde{E}$ (4p) Rydberg states were also observed and reassigned in the present REMPI spectrum. The $\tilde{E}$ (4p) band origin of 62025 cm^{-1} assigned here agrees well with that previously observed by (3+1) REMPI spectrum.[23] The irregular intervals along the higher levels of the 1_0^n ($n \geq 2$) in the $\tilde{E}$ (4p) Rydberg state have been clarified by our incompletely rotationally resolved REMPI spectrum. The $\tilde{E}$ (4p) Rydberg state appears to be perturbed by a crossing with the $\tilde{F}$ state ($\nu_{0-0} = 63812$ cm^{-1}). Most probably, the $\tilde{F}$ state is another hybrid state of 4p Rydberg series with a quantum defect of 1.50. The 4p Rydberg orbitals possess three symmetries: $b_1(4p_x)$, $b_2(4p_y)$, and $a_1(4p_z)$, which give rise to the state symmetries of $^1A_1$,$^1A_2$, and $^1B_1$. The present work cannot reveal the symmetries of the $\tilde{E}$ (4p) and $\tilde{F}$ states.

The (2+1) REMPI spectrum of the $\tilde{E}$ (4p) state displays an extremely strong progression in this study. Accordingly, we expected that a *np* Rydberg series should appear in the (2+1) REMPI spectrum. For example, the Rydberg formula predicts that the 5p Rydberg state should fall within the energy range of 71220−72340 cm^{-1} (276.5−280.8 nm). We have paid careful attention to investigate the 5p Rydberg state. However, two-photon resonant bands associated with the 5p Rydberg state have not been found. The most like explanation for this "missing" state may be that the 5p state is heavily predissociative or correlative to the lower dissociative states. In fact, as shown in Figure 5, the intensity of the SF_2 ion signal in the range of 272−282 nm, which was associated with the higher vibrational progressions $1_0^{\upsilon'}(\upsilon' \geq 3)$ of the 5s and 3d Rydberg states, decrease sharply. This evidence may support the above explanation. In addition, unfavorable Franck−Condon factors may also prevent us from observing these "missing" states. Therefore, even if they exist, it seems very difficult to observe them.

TABLE 5: Summary of the Electronic Band Systems and the Spectroscopic Constants of the SF_2 Radical Observed by Previous and Present Study

electronic states	T_0 (cm^{-1})	quantum defect[a]	ω_1 (a_1) (cm^{-1})	ω_2 (a_1) (cm^{-1})
$\tilde{A}\ ^1B_1$	18 200[b]			
$\tilde{B}'\ ^1A_1$	38 623			
$\tilde{B}\ ^1B_1(4s)$	54 470[d]	1.98	981(23)	388(24)
	54 433[c]	1.98[c]	991(12)[c]	361(24)[c]
$\tilde{C}\ ^1A_2$	56 219−61 278			
	57 000−60 000[c]			
$\tilde{E}$ (4p)	62 025	1.61	941(27)	413(12)
	62 015[c]	1.61[c]	931(59)[c]	383(42)[c]
$\tilde{F}$	63 812	1.50	966(6)	417(23)
$\tilde{G}$ (3d)	68 378	0.086	939(12)	
$\tilde{H}$ (3d)	68 571	0.064	936(4)	
$\tilde{I}$ (3d)	68 847	0.032	933(4)	
$\tilde{J}\ ^1B_1(5s)$	68 951	2.01	942(3)	

[a] Based upon $IP_a = 81301$ cm^{-1} from ref 22. [b] From ref 21. [c] From ref 23. [d] Origin derived by the extrapolation.

The $\tilde{G}$, $\tilde{H}$, and $\tilde{I}$ states shown in Figure 8 comprise the *nd*-Rydberg series. The $\tilde{G}$ (3d), $\tilde{H}$ (3d), and $\tilde{I}$ (3d), lying at 68378, 68571, and 68847 cm^{-1}, respectively, are three different hybrid states of the 3d Rydberg series. The 3d Rydberg orbitals are of symmetries a_1, a_2, b_2, b_1, and a_1, which result in the state symmetries of $^1B_1$, $^1B_2$, $^1A_2$, $^1A_1$, and $^1B_1$, respectively. The symmetries of the $\tilde{G}$ (3d), $\tilde{H}$ (3d), and $\tilde{I}$ (3d) cannot be described.

Figure 8 shows three valence electronic states of the SF_2 radical. The first excited electronic state, $\tilde{A}^1B_1$, was observed by the previous emission spectrum,[21] which arises from the promotion of the $3b_1$ electron into the $9a_1$ orbital with the configuration: $...5b_2^2 8a_1^2 3b_1^1 9a_1^1$ ($\tilde{A}\ ^1B_1$). The $\tilde{C}$ state was observed by the previous[23] and present (2+1) REMPI spectrum. The $\tilde{C}$ state resides between 56219−61278 cm^{-1}. The most like configuration and symmetry of the $\tilde{C}$ state may be described as

$$... 5b_2^2 8a_1^2 3b_1^1 6b_2^1\ \tilde{C}\ (^1A_2)$$

More recently, our (1+1+1) REMPI spectrum showed that a low valence state (labeled as $\tilde{B}'$ state) resides in the range of 38600−42350 cm^{-1}. Its band origin locates at 38623 cm^{-1}. The detailed investigation is in progress.

Table 5 lists the known electronic band systems and the spectroscopic constants of the SF_2 radical observed by previous and this work. The progressions of the present REMPI bands exhibit that the frequency intervals of the Rydberg states are similar to the vibrational frequency of 935(40) cm^{-1} appeared in the ground-state cation.[22] This similarity is expected of a Rydberg state that possesses a ground-state cation core. Furthermore, the SF stretching frequencies $\omega_1'(a_1)$ for the Rydberg states are ~100 cm^{-1} greater than the $\omega_1'' = 840$ cm^{-1} observed in the ground state of neutral SF_2 radical.[19] The increasing of the vibrational frequencies in Rydberg states may indicate that the S−F bond is strengthened.

B. Ionization Potential of SF_2 Radical. The Rydberg series formed from the ns^1B_1 band origins enable a direct determination of the first adiabatic ionization potential of the SF_2 radical. The best fit of $\tilde{B}\ ^1B_1(4s)$ and $\tilde{J}\ ^1B_1(5s)$ Rydberg state origins yields

a quantum defect of $\delta = 1.961(6)$ and an ionization potential of 80830(4) cm^{-1} ($IP_a = 10.021(1)$ eV).

Prior to this work, two groups have measured the IP_a value using photoelectron spectroscopy, and given the value of 10.08 $\pm$ 0.05 eV[22] and 10.29 $\pm$ 0.30 eV,[32] respectively. More recently, the ionization potential of 10.15 $\pm$ 0.19 eV was derived from ab initio calculations.[33] In this work, the value of the IP_a for SF_2 radical agrees closely with the $IP_a = 10.08(5)$ eV reported by De Leeuw et al.[22] and the theoretical value of 10.15-(19) eV.[33] Because the IP_a value in the work is based upon the assigned spectra of several states, the agreement of IP_a between ours and previous data in turn enhanced the confidence in the present assignments.

C. Pulsed Free Radical Source. In this paper, we reported a pulsed radical source, which was formed by a pulsed dc electric discharge in a pulsed supersonic beam. The use of an electric discharge for preparation of the transient species is a traditional technique, which has proved as a useful technique for the spectroscopic studies.[3−10] This radical production method bears many appealing aspects, such as (1) its generality, (2) generating a cooled precursor with a supersonic expansion beam, and (3) simply operating at flexible pressure. Our design is somewhat similar to that of Rosser et al.[9] The difference between the two approaches is the discharge design. For example, a laser discharge mode was used to increase the stability of the discharge and the discharge fired in the supersonic beam avoided the free radicals to be quenched by other species. In our experiment, a stable radical source with high density was set up and the background ions generated by the dc discharge were efficiently eliminated. Definitely, the pulsed radical source is also accessible to LIF measurement for free radicals.

Acknowledgment. We thank the National Natural Foundation, National Education Committee Foundation, and National Climbing Plan Foundation of China for financial supports. We also thank Mr. Hongfa Lin and Mr. Hui Gao for their helpful assistance during the establishment of the experimental apparatus.

References and Notes

(1) Hudgens, J. W. *Advanced in Multiphoton Processes and Spectroscopy*; Lin, S. H., Ed.; World Scientific: Singapore, 1988; Vol. 4, p 171−295.

(2) Ashfold, M. N. R.; Clement, S. G.; Howe, J. D.; Western, C. M. *J. Chem. Soc., Faraday Trans.* **1993**, *89*, 1153.

(3) Droege, A. T.; Engelking, P. C. *Chem. Phys. Lett*. **1983**, *96*, 316.

(4) Sharpe, S.; Johnson, P. M. *Chem. Phys. Lett.* **1984**, *107*, 35. *J. Mol. Spectrosc.* **1986**, *116*, 247.

(5) Bramble, S. K.; Hamilton, P. A. *Chem. Phys. Lett*. **1990**, *170*, 107.

(6) Qingzhang, Lu; Yang Chen; Xingxiao, Ma; et al. *Chem. Phys. Lett*. **1991**, *178*, 51.

(7) Jouvet, C.; Dedonder, C. L.; Solgadi, D. *Chem. Phys. Lett.* **1989**, *156*, 569.

(8) Schlackta, R.; Lask, G.; Tsay, S. H.; Bondybey, V. E. *Chem. Phys.* **1991**, *155*, 267.

(9) Rosser, K. N.; Wang, Q. Y.; Western, C. M. *J. Chem. Soc., Faraday Trans.* **1993**, *89*, 391.

(10) Booth, J. P.; Hancock, G.; Toogood, M. J.; Mckendrick, K. G. *J. Phys. Chem*. **1996**, *100*, 47.

(11) d'Agostino, R.; Flamm. D. L. *J. Appl. Phys*. **1981**, *52*, 162.

(12) Janssenn, F. J.; Kema, J. G. *Sci. Tech. Rep*. **1984**, *2*, 9.

(13) Griffin, G. D.; Easterly, C. E.; Sauers, I.; Ellis, H. W.; Christophorou, L. G. *Tox. Environ. Chem*. **1984**, *9*, 139.

(14) Ryan, K. R.; Plumb, I. C. *Plasma Chem. Plasma Process.* **1988**, *8*, 263.

(15) Johnson, D. R.; Powell, F. X. *Science* **1969**, *164*, 950.

(16) Kirchhoff, W. H.; Johnson, D. R.; Powell, F. X. *J. Mol. Spectrosc*. **1973**, *48*, 157.

(17) Endo, Y.; Saito, S.; Hirota, E. *J. Mol. Spectrosc.* **1979**, *77*, 222.

(18) Haas, A.; Willner, H. *Spectrochem. Acta* **1978**, *34A*, 541.

(19) Deroche, J. C.; Burger, H.; Schulz, P.; Willner, H. *J. Mol. Spectrosc.* **1981**, *89*, 269.

(20) Willner, H. Z. *Anorg. Allg. Chem*. **1981**, *481*, 117.

(21) Glinski, R. J.; Taylor, C. D. *Chem. Phys. Lett.* **1989**, *155*, 511.

(22) De Leeuw, D. M.; Mooyman, R.; de Lange, C. A. *Chem. Phys.* **1978**, *34*, 287.

(23) Johnson, R. D., III; Hudgens, J. W. *J. Phys. Chem.* **1990**, *94*, 3273.

(24) Striganov, A. R.; Sventitskii, N. S. *Tables of Spectal Lines of Neutral and Ionized Atoms*; Plenum: New York, 1968.

(25) King, O. S.; Schenck, P. K.; Travis, J. C. *Appl. Opt.* **1977**, *16*, 2617.

(26) Hudgens, J. W.; Johnson, R. D., III; Tsai, B. P.; Kafafi, S. A. *J. Am. Chem. Soc.* **1990**, *112*, 5763.

(27) Hudgens, J. W.; Dulcey, C. S.; Long, G. R. *J. Chem. Phys.* **1987**, *87*, 4546.

(28) Johnson, R. D., III; Tsai, B. P.; Hudgens, J. W. *J. Chem. Phys*. **1989**, *91*, 3340.

(29) Howe, J. D.; Ashfold, M. N. R.; Western, C. M.; Hudgens, J. W. *J. Chem. Phys.* **1996**, *104*, 2789.

(30) Manson, S. T. *Phys. Rev.* **1969**, *182*, 97.

(31) In these two-photon experiments the vibrational selection rules are identical to those of one-photon experiments as long as the vibration−electronic interaction is small. See: Herzberg, G. *Molecular Spectra and Molecular Structure*; Van Nostrand. Reinhold: New York, 1966; Vol. III, p 150.

(32) Chase, M. W. *J. Phys. Chem. Ref. Data* **1995**, (Suppl. 1.) 14.

(33) Irikura, K. K. *J. Chem. Phys*. **1995**, *102*, 5357.